CubeSat Mass Spectrometer

Stojan Madzunkov, Viktor Hristov, Anton Belousov, Dragan Nikolic, Jurij Simcic, Kelsey L Reichenbach, Wesley Faistenhammer, Declan Winship, Bret Bronner, Rok Mesar, Crt Valentincic and Jason Feldman

National Aeronautics and Space Administration
Jet Propulsion Laboratory
California Institute of Technology

CubeSat MS

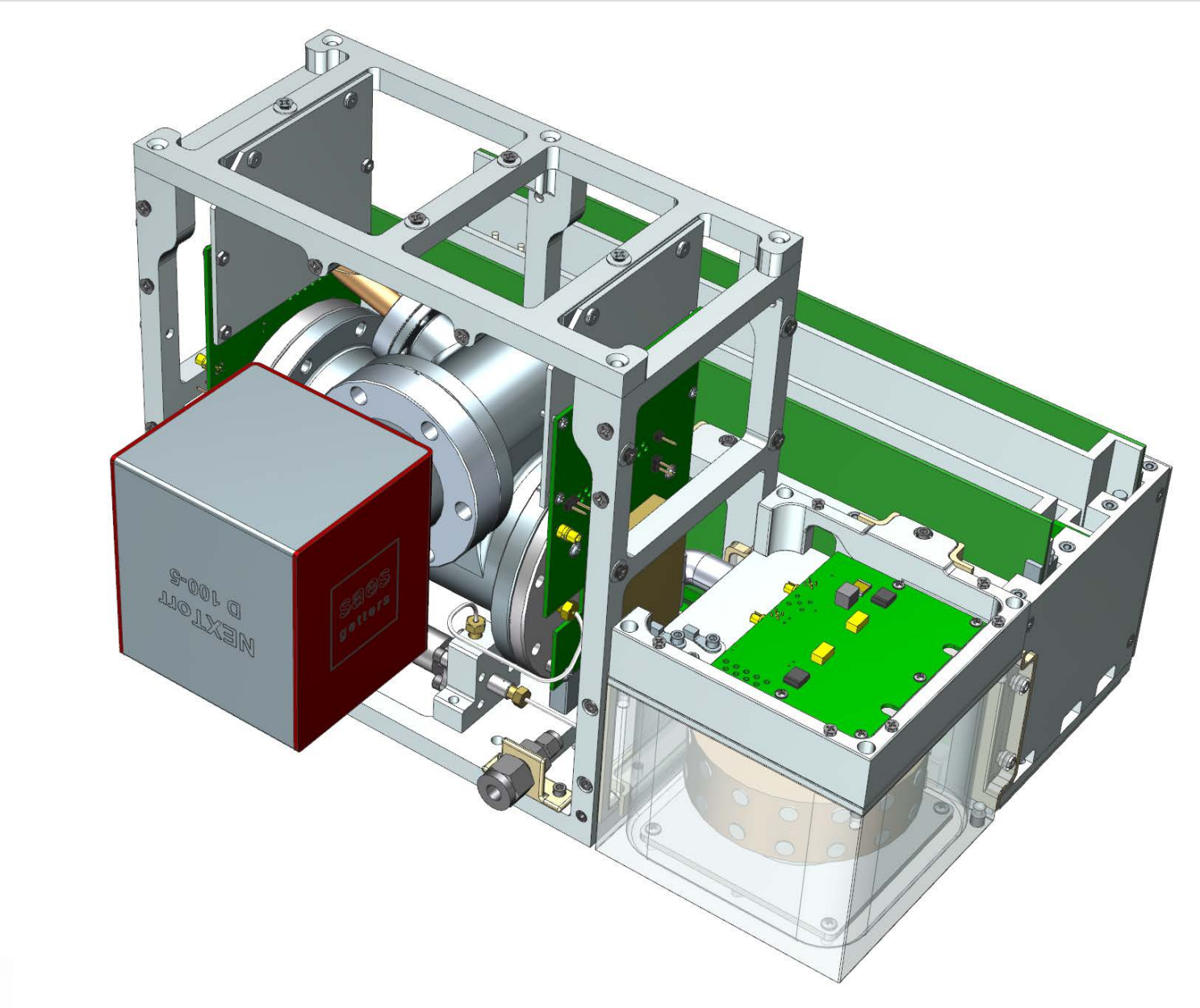

Science

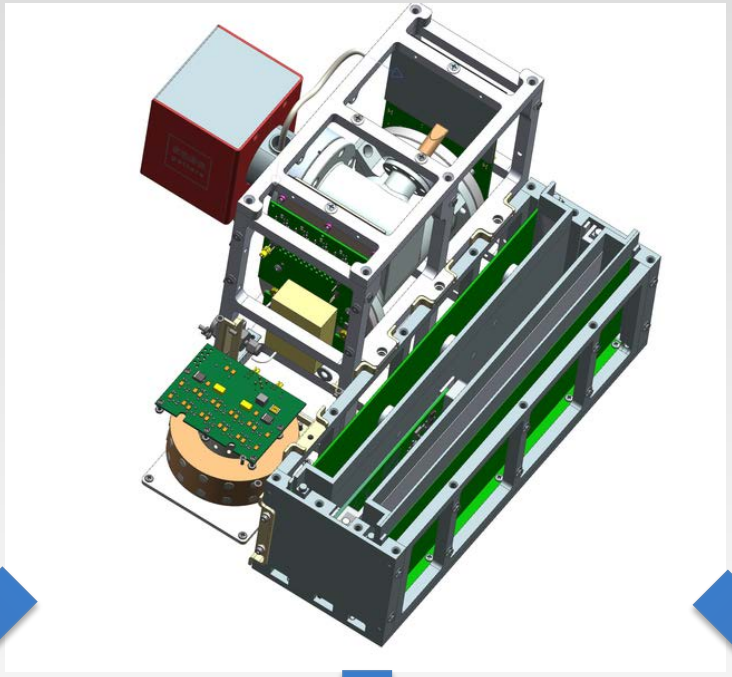

Atmosphere profiling
High repetition rate
full range measurements

Geochronology
Accurate noble
gas measurements

Life detection
Biosignatures
Amino and fatty acids
MS/MS

Kr/Xe calibrated aliquots*

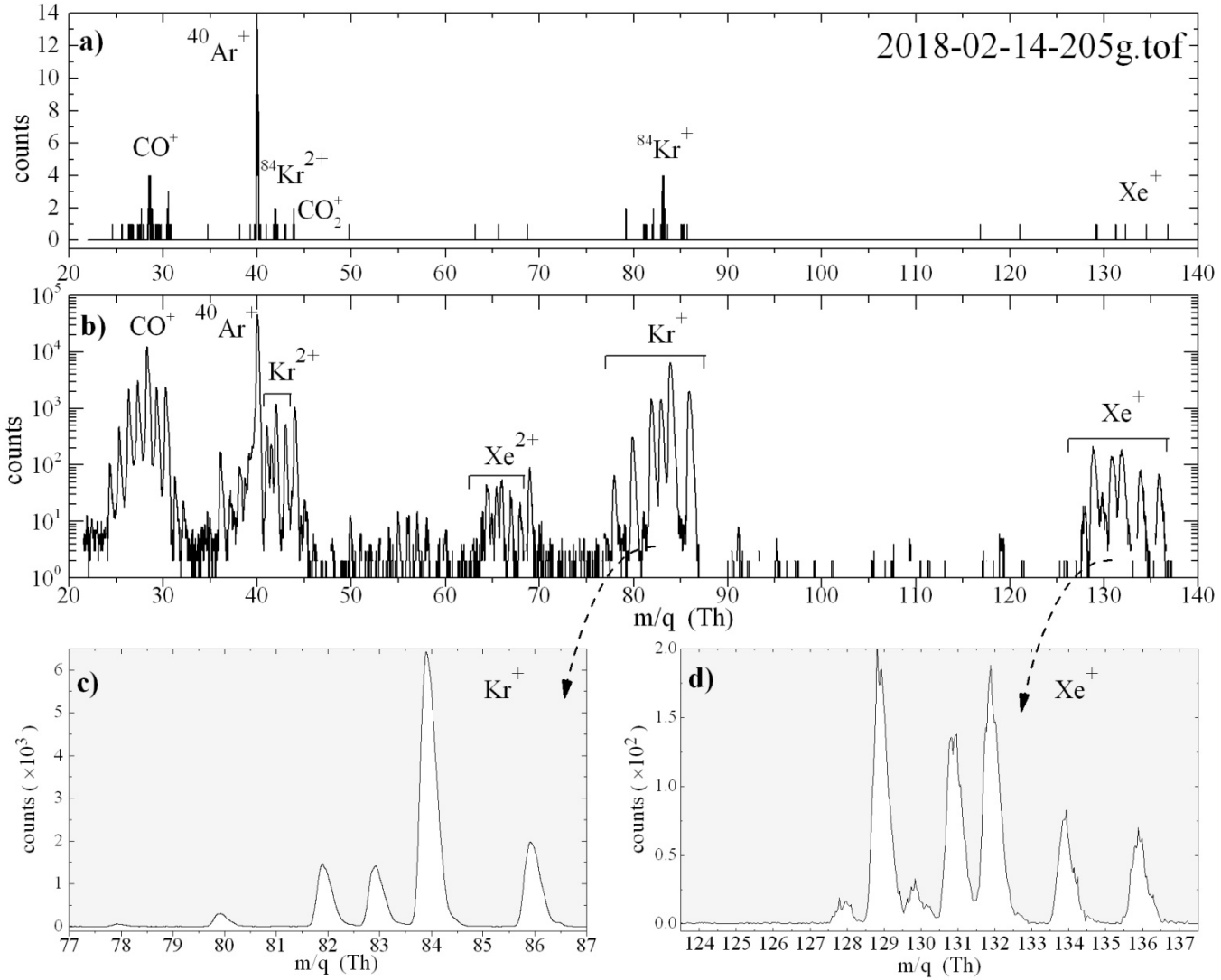

Figure XX: Isotope spectra of an aliquot of calibrating gas (1.7E-10 Torr of Kr and 1.3E-11 Torr of Xe) measured continuously for 7 hours yielded a 0.6 ‰ precision on the 86Kr/84Kr ratio; (a) the QITMS signal acquired in 50ms; (b)) the QITMS signal in log scale acquired in 1min; (c) same as (b) but in linear scale and for Kr multiplet only; (d) same as (b) but in linear scale for Xe multiplet; contribution from singly and doubly charged Kr and Xe ions are clearly visible after 1min; sample contamination by leaked environmental air show Ar (not pumped in static mode), and CO2 polutant fragments (pumped in static mode by getter pump).

*G. Avice, A. Belousov, K. A. Farley, S. M. Madzunkov, J. Simcic, D. Nikolić, M. R. Darrach, C. Sotin, **High-precision measurements of krypton and xenon isotopes with a new static-mode Quadrupole Ion Trap Mass Spectrometer,** *Journal of Analytical Atomic Spectrometry (2018).*

QITMS has counting statistics that follows Poisson Distribution

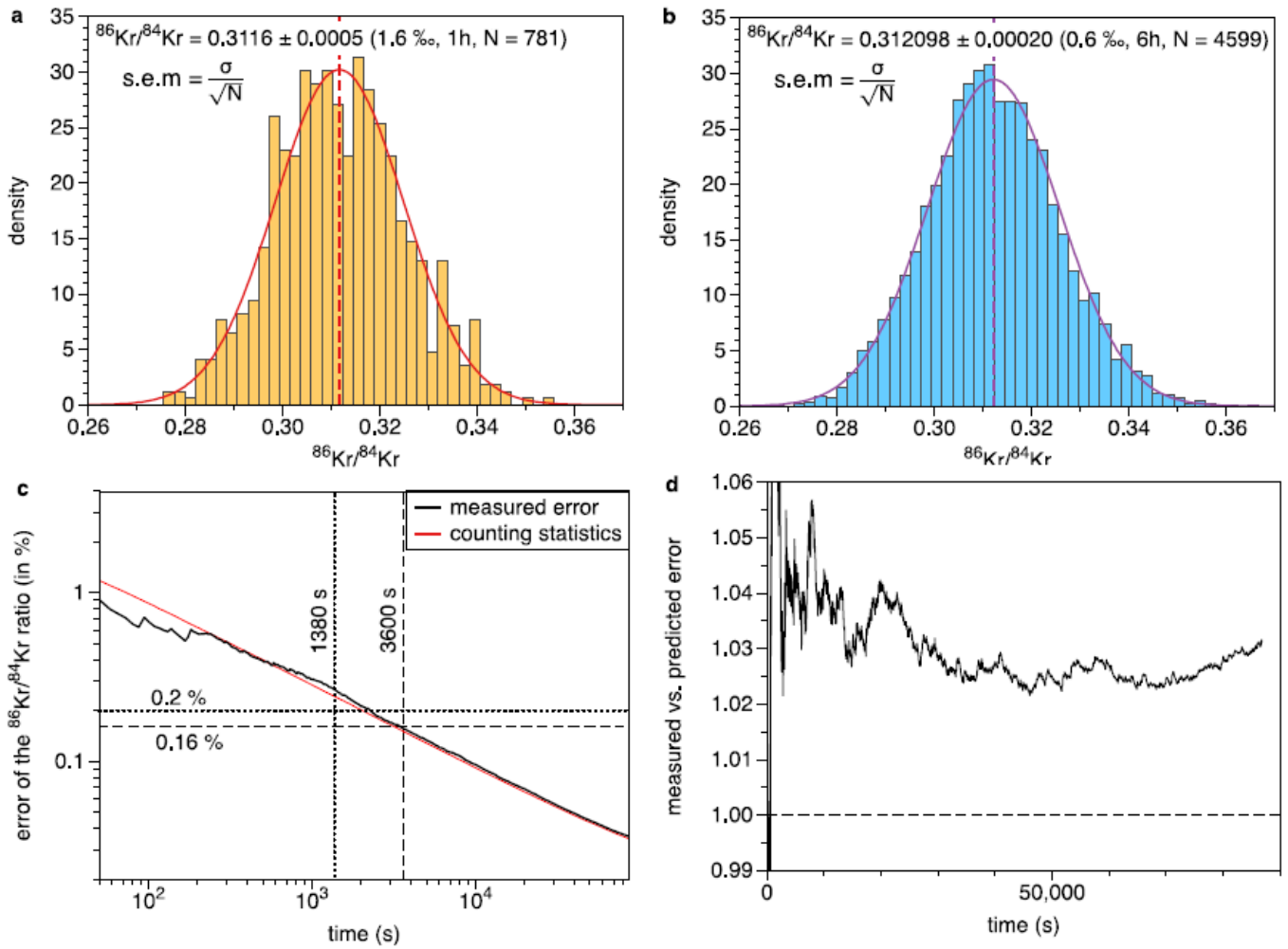

Figure XXX: (a) Distribution of the 86Kr/84Kr ratios (in N=781 sets, each containing 92 frames 50ms in duration) for 1hour of static measurement of an aliquot of the standard gas. Ratios are distributed following a Poisson distribution (red curve) centered at 0.3116 (dashed line) with 1.6‰ accuracy. (b) Distribution of the 86Kr/84Kr ratios (in N=4599 sets, each containing 94 frames 50ms in duration) for 6hours of static measurement on another aliquot of the standard gas, where accuracy reached 0.6 ‰. (c) Evolution of the error on the 86Kr/84Kr ratio with the accumulation of isotope ratios for a 24hour measurement. The measured error closely follows the error predicted when only counting statistics (Poisson's law) is considered (red curve). The black dashed lines correspond to the case presented in (a). The dotted line offers a comparison with the performance of a magnetic sector instrument. (d) Time evolution of the ratio between the measured error and the error predicted by Poisson counting statistics alone, showing measured error to be few percent higher than the theoretical error.

long-term reproducibility of QITMS measurements

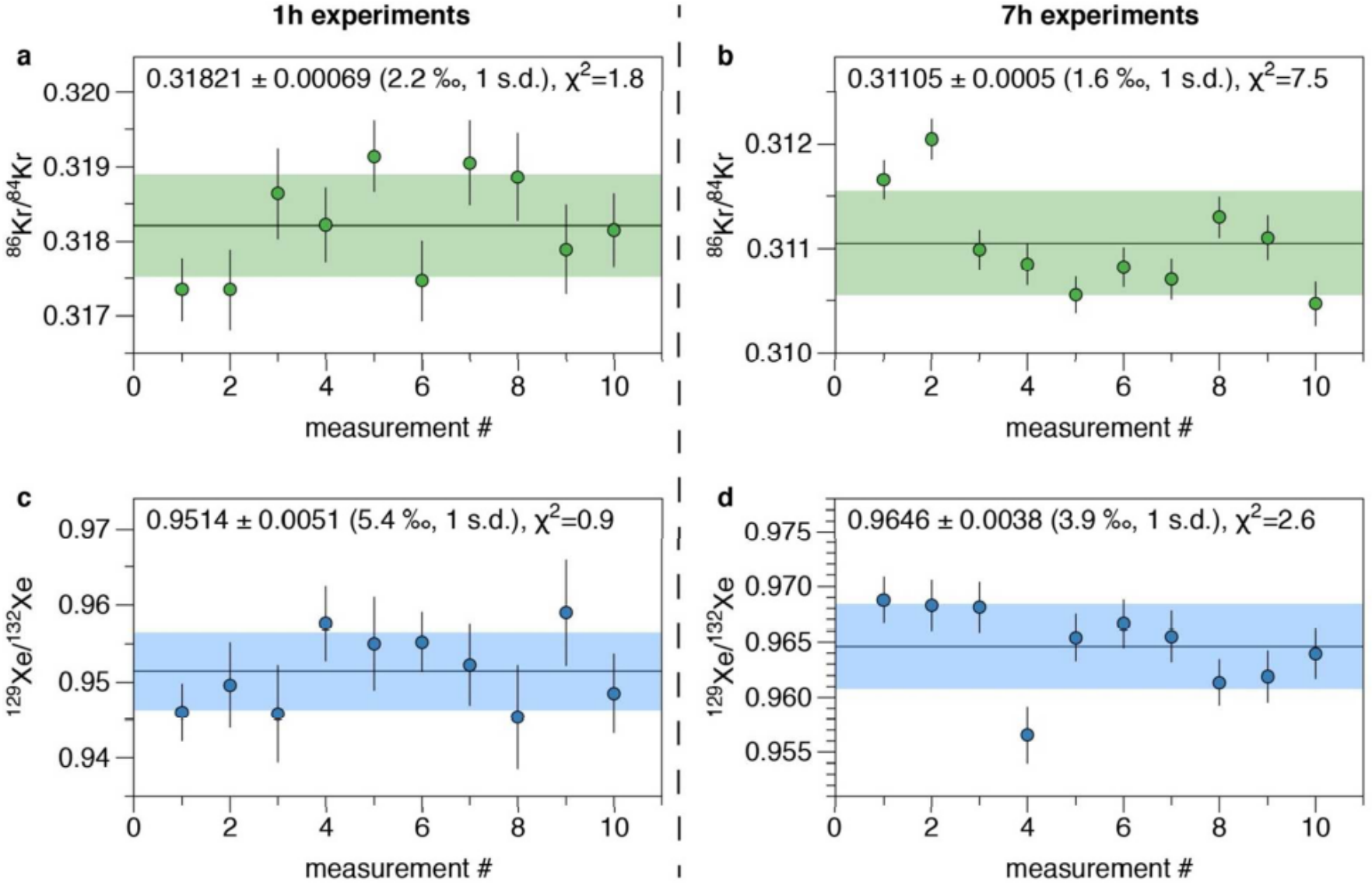

Figure XXXX: Reproducibility of the instrument for 86Kr/84Kr and 129Xe/132Xe ratios characterized through 10 independent measurements of varying duration but set apart by 1hour of idle period; (a) 86Kr/84Kr ratios when 10 measurements were 1hour long; (b) 86Kr/84Kr ratios for 10 measurements each 7hours long; (c) same as (a) but for 129Xe/132Xe ratios; (d) same as (b) but for 129Xe/132Xe; Error bars for each dataset is the 1σ standard deviation.

Isotopic composition of Kr measured in zircons by QITMS

The zircon measured in this study is from high-grade metamorphic terrains in northern Sri Lanka. The age of metamorphic resetting of this terrain is ~600 Ma and zircons typically contain high concentration of uranium (1000 ppm) and as a result Xe and Kr isotopes produced by spontaneous fission of 238U have been accumulating in the zircon for the last ~600 Ma. Gas from 600mg of a single zircon megacryst was extracted at Caltech in a resistance furnace in the presence of lithium tetraborate. QITMS is capable of clearly separating both major and minor isotopic ratios in zircons from the those measured in the ambient Air.

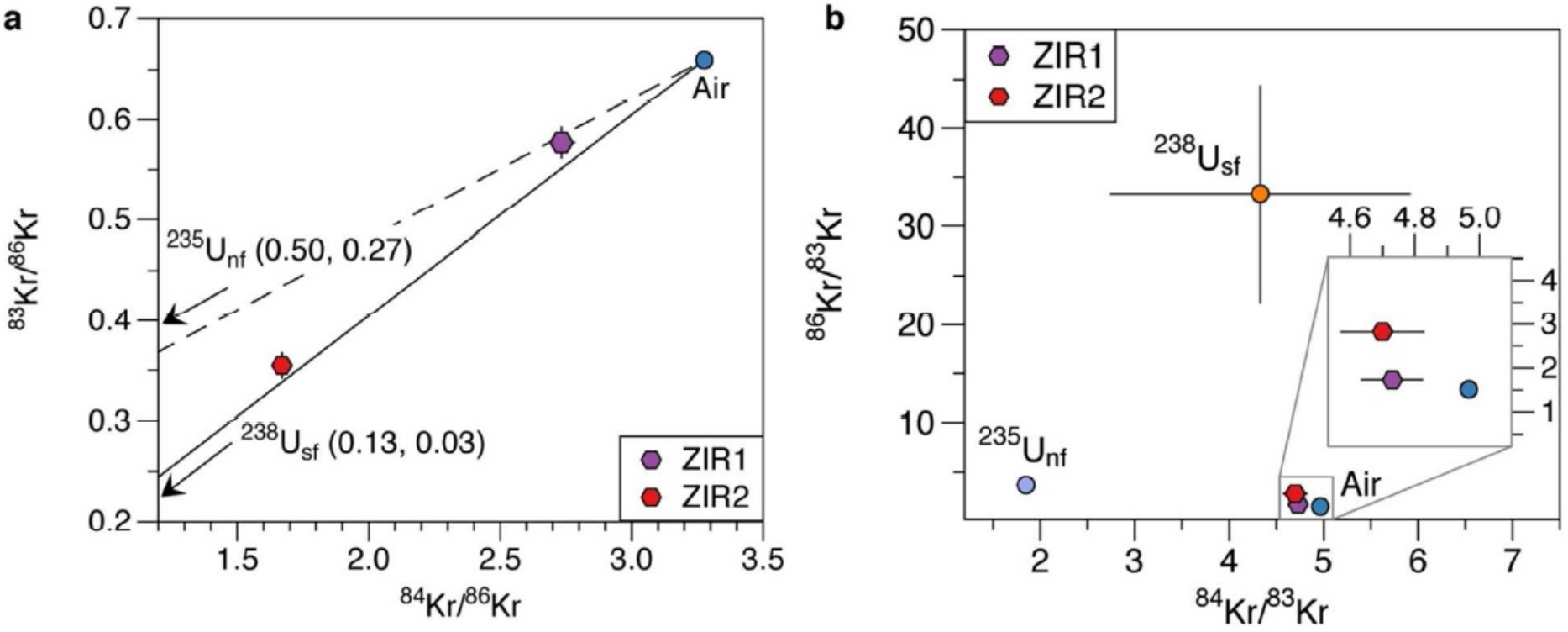

Figure XXXXX: Isotopic composition of Kr measured in two different zircons with 1σ error bars; Three-isotope diagrams: (a) showing a clear contribution either from the spontaneous fission of 238U (238Usf) or from the neutron-induced fission of 235U (235Unf), and (b) in another dimensional space showing the distinct isotope composition for 238Usf and 235Unf. Inset is the measured isotope composition in ambient Air.

Model of the measurement concept

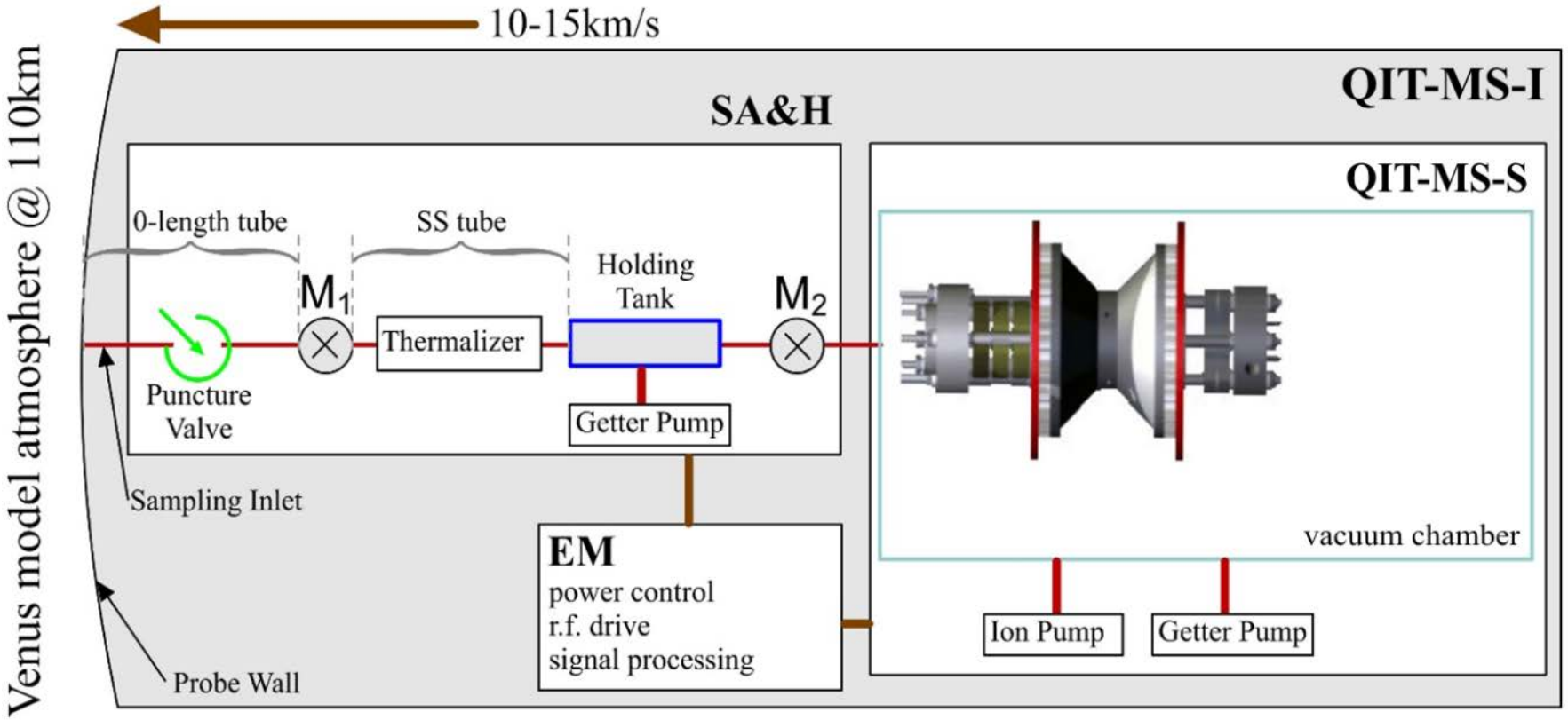

Computational Model

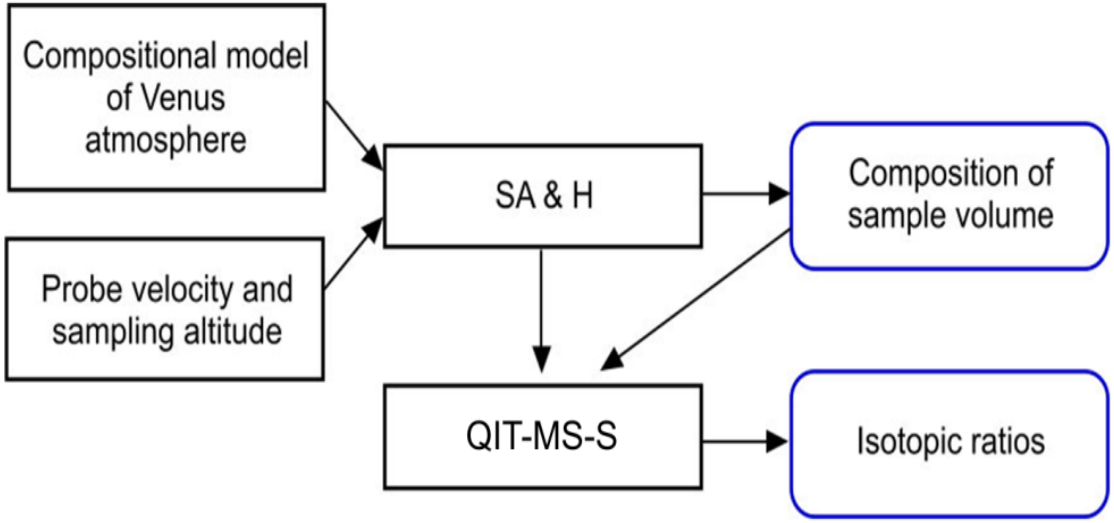

Figure 2: Simulation flow chart : Inputs to the SA&H module are the composition of the Venus atmosphere and the probe trajectory. Intermediary product from the SA&H module is the composition of the sample volume, that is fed to the QIT-MS-S module for the mass spectrum generation and determination of isotopic ratios of noble gases.

sampling altitude z(t) and probe velocity v

$$z(t) = z_{\min} + \Delta z \cdot \left(\frac{x(t)}{a} - 1\right)^2$$

$$v \cdot (t - t_{\text{avr}}) = \frac{a}{2}\sqrt{1 + \left(\frac{2\Delta z}{a} \cdot \left(\frac{x(t)}{a} - 1\right)\right)^2} \cdot \left(\frac{x(t)}{a} - 1\right) + \frac{a^2}{4\Delta z}\sinh^{-1}\left(\frac{2\Delta z}{a} \cdot \left(\frac{x(t)}{a} - 1\right)\right)$$

the probe trajectory z(t) is a shallow parabolic arc with the highest and the lowest altitudes at zmax=112km and zmin=110km, respectively.

the probe velocity v=10.87km/s is kept constant and horizontal displacement x(t) is numerically determined from the above system of equations.

Analysis of isotopic abundances in noble gases

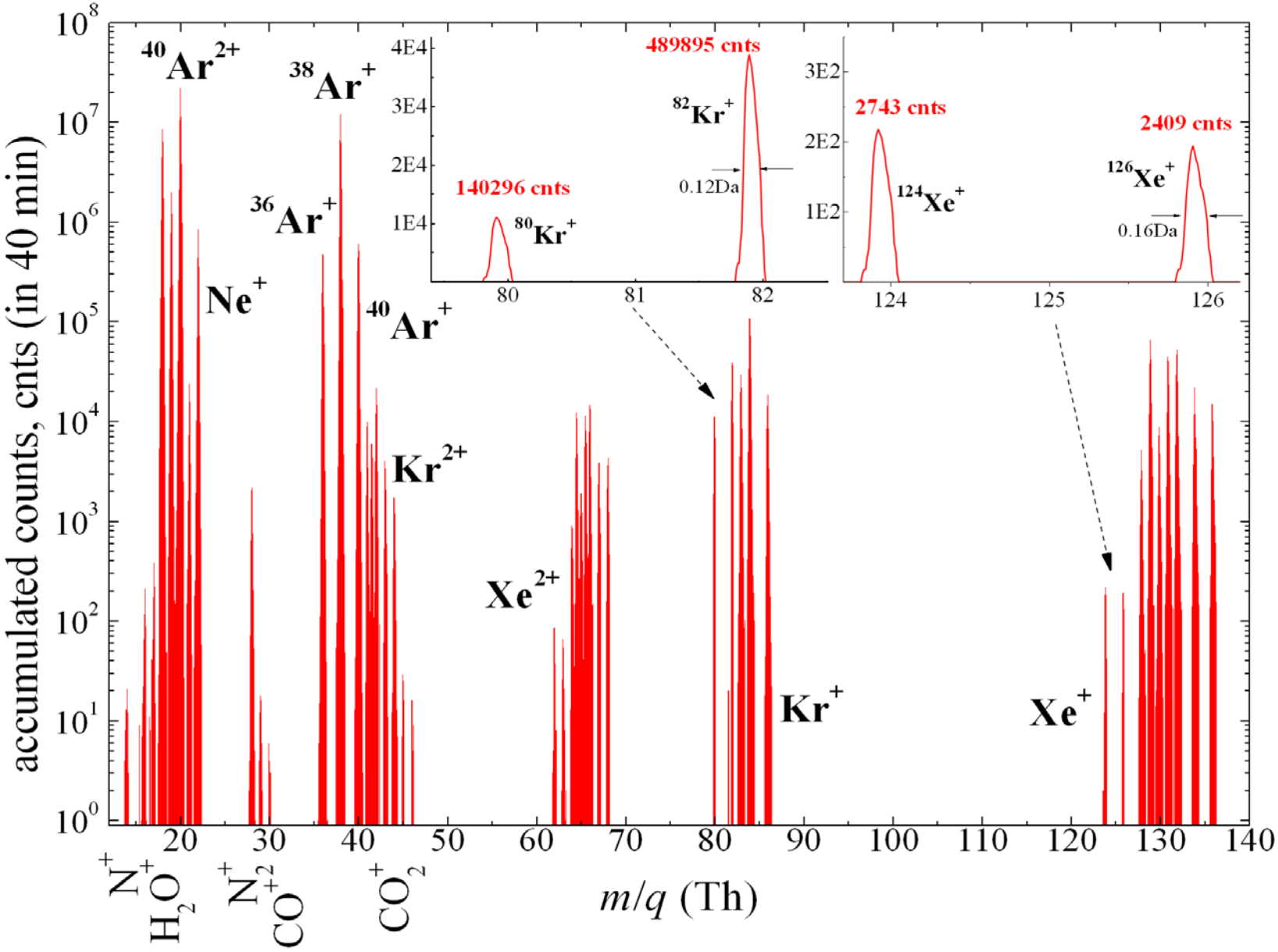

Figure 4: Synthetic mass spectra of noble gases at 10mTh bin resolution.

CubeSat MS Concept

3D printed titanium vacuum chamber

Ion & Getter pump

QIT Sensor

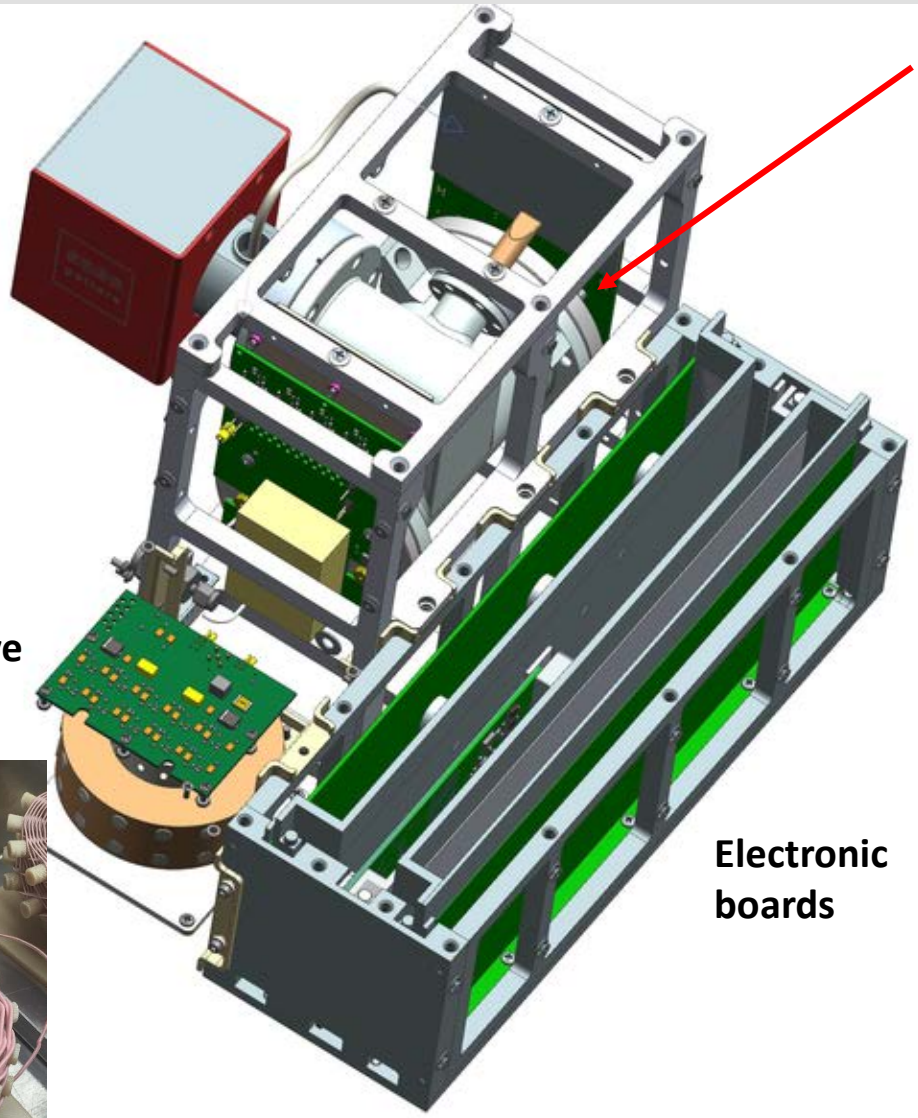

High Q diamond weave Litz wire coil

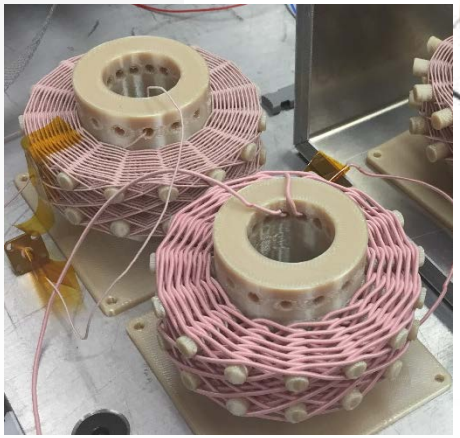

Electronic boards

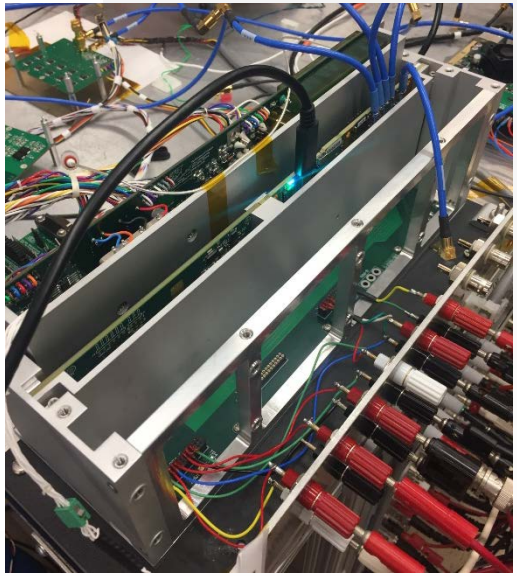

CubeSat MS Concept – QIT Sensor

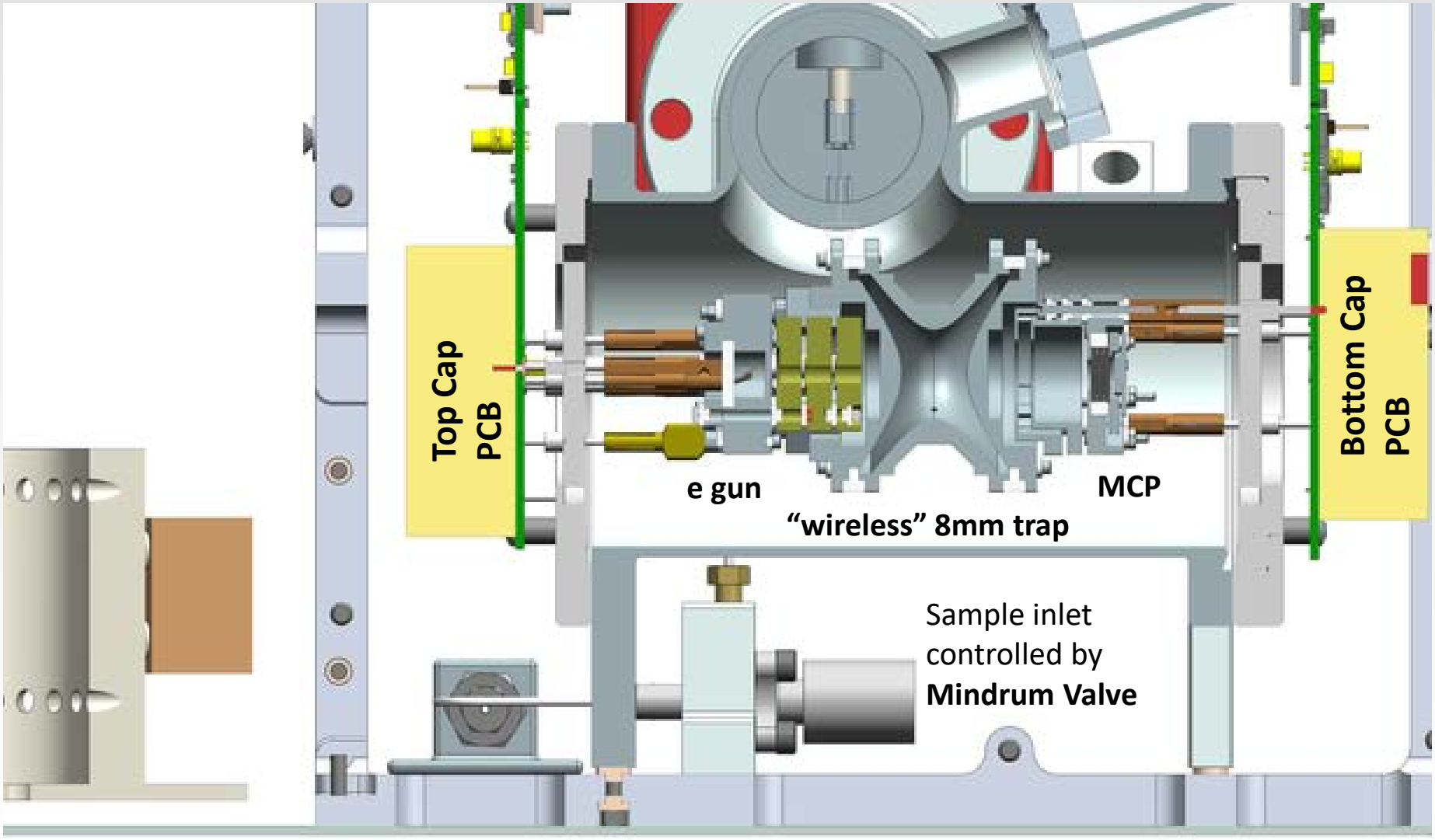

Backplane

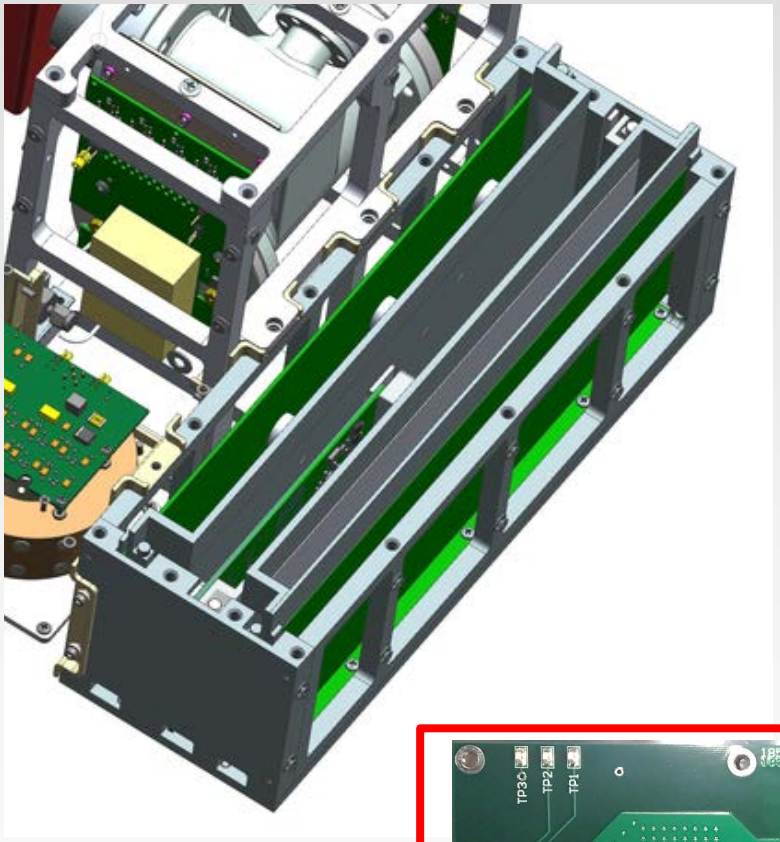

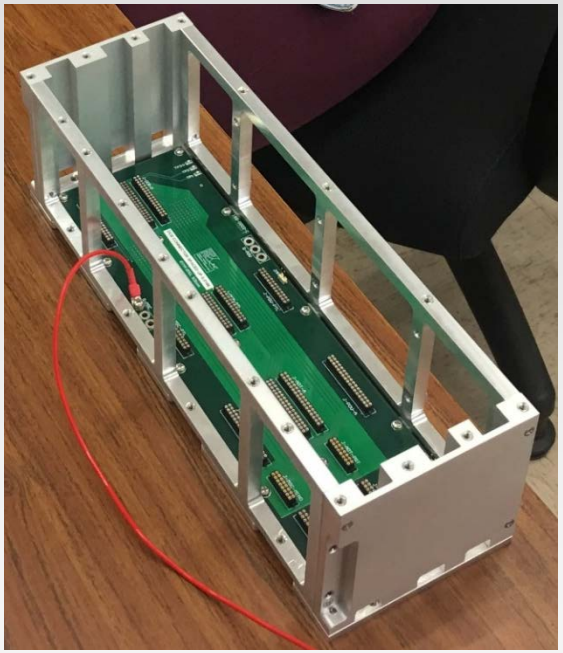

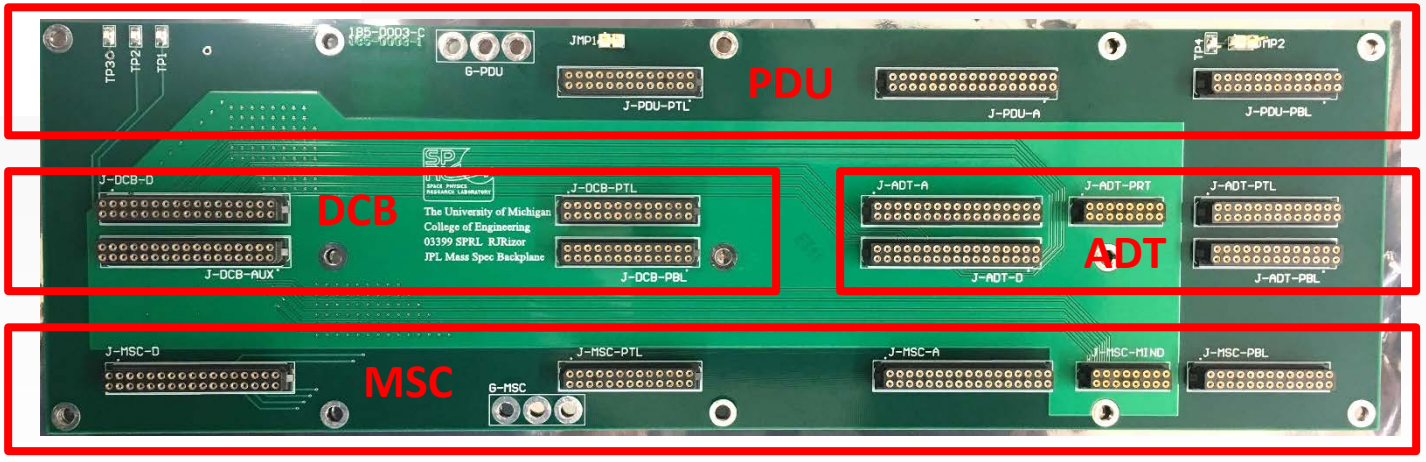
PDU
G-PDU
J-PDU-PTL
J-PDU-A
J-PDU-PBL
DCB
J-DCB-D
J-DCB-AUX
J-DCB-PTL
J-DCB-PBL
The University of Michigan
College of Engineering
03399 SPRL RJRizor
JPL Mass Spec Backplane
ADT
J-ADT-A
J-ADT-PRT
J-ADT-PTL
J-ADT-D
J-ADT-PBL
MSC
J-MSC-D
G-MSC
J-MSC-PTL
J-MSC-A
J-MSC-MIND
J-MSC-PBL

Digital Control Board (DCB) and Analog Digital Telemetry (ADT) boards

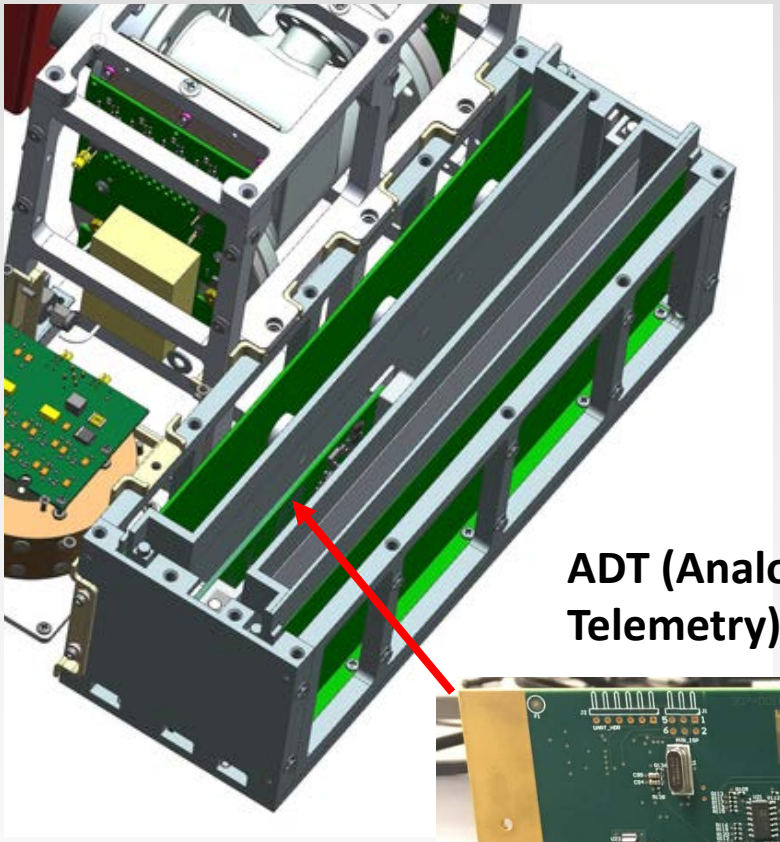

DCB (Digital Control Board)

- Dual ARM Cortex-A9 System On Chip FPGA
- Data acquisition
- RF generation
- Electronics control

ADT (Analog Digital Telemetry)

ADT and DCB heatsink

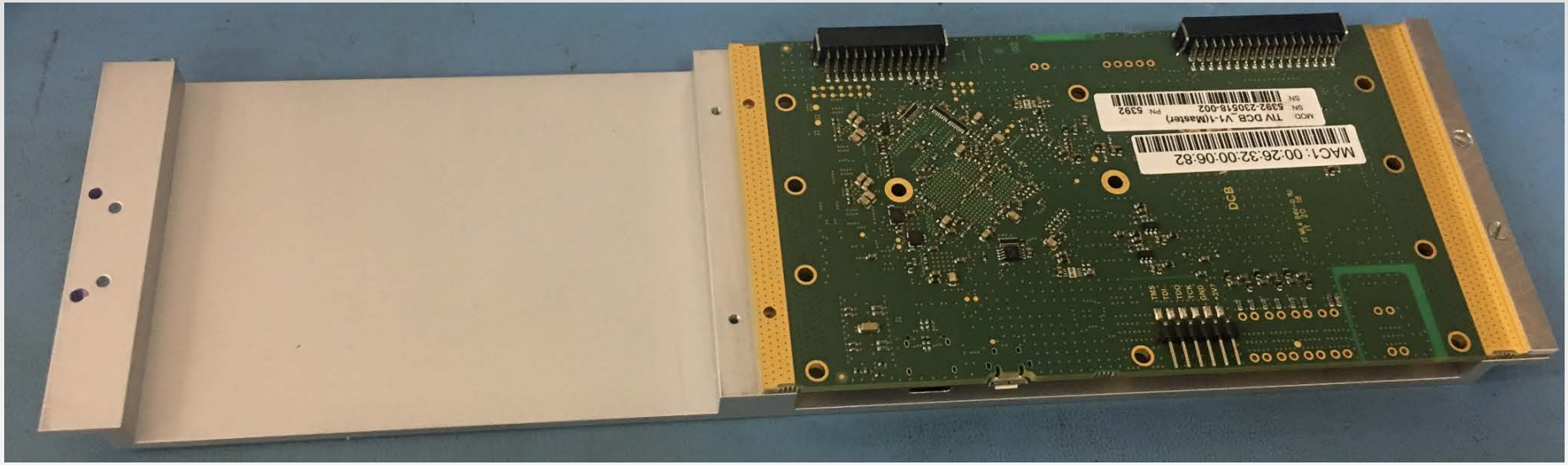

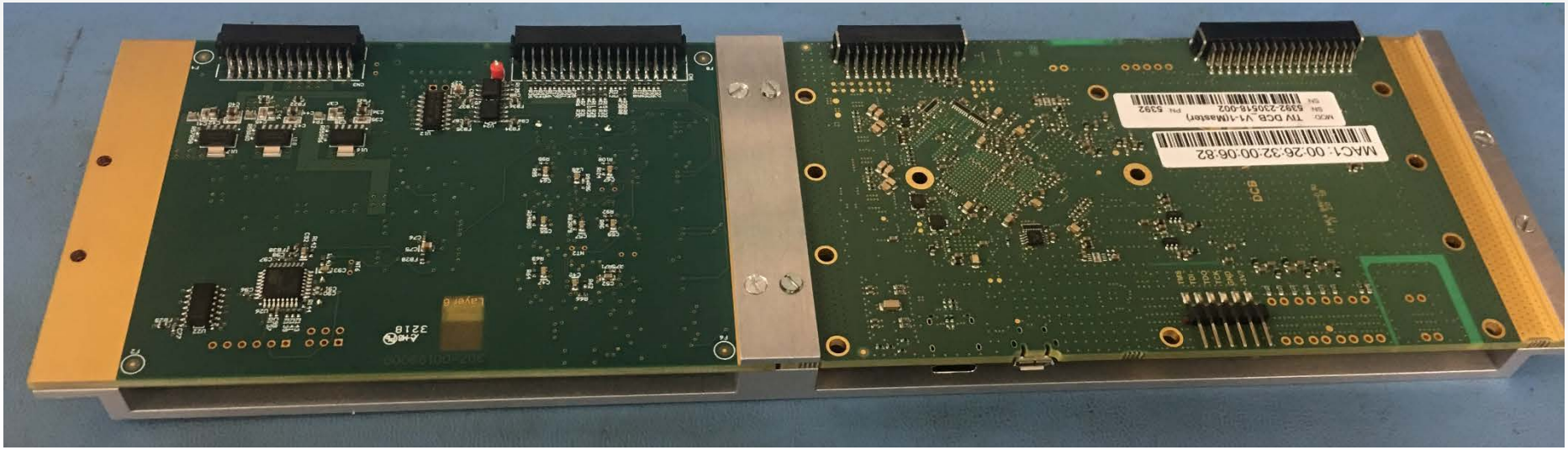

DCB and ADT

Samtec Circular RF Shielded Twisted Pair Twinax Cable:

- 100 ohm differential pair signal routing
- 28 AWG shielded twisted pair cable

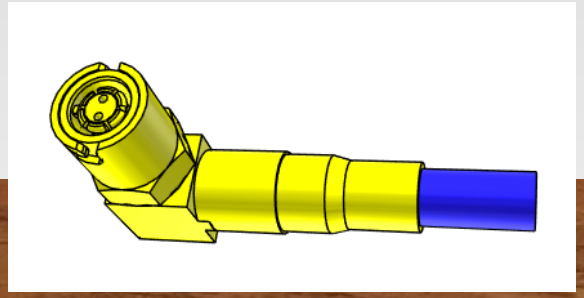

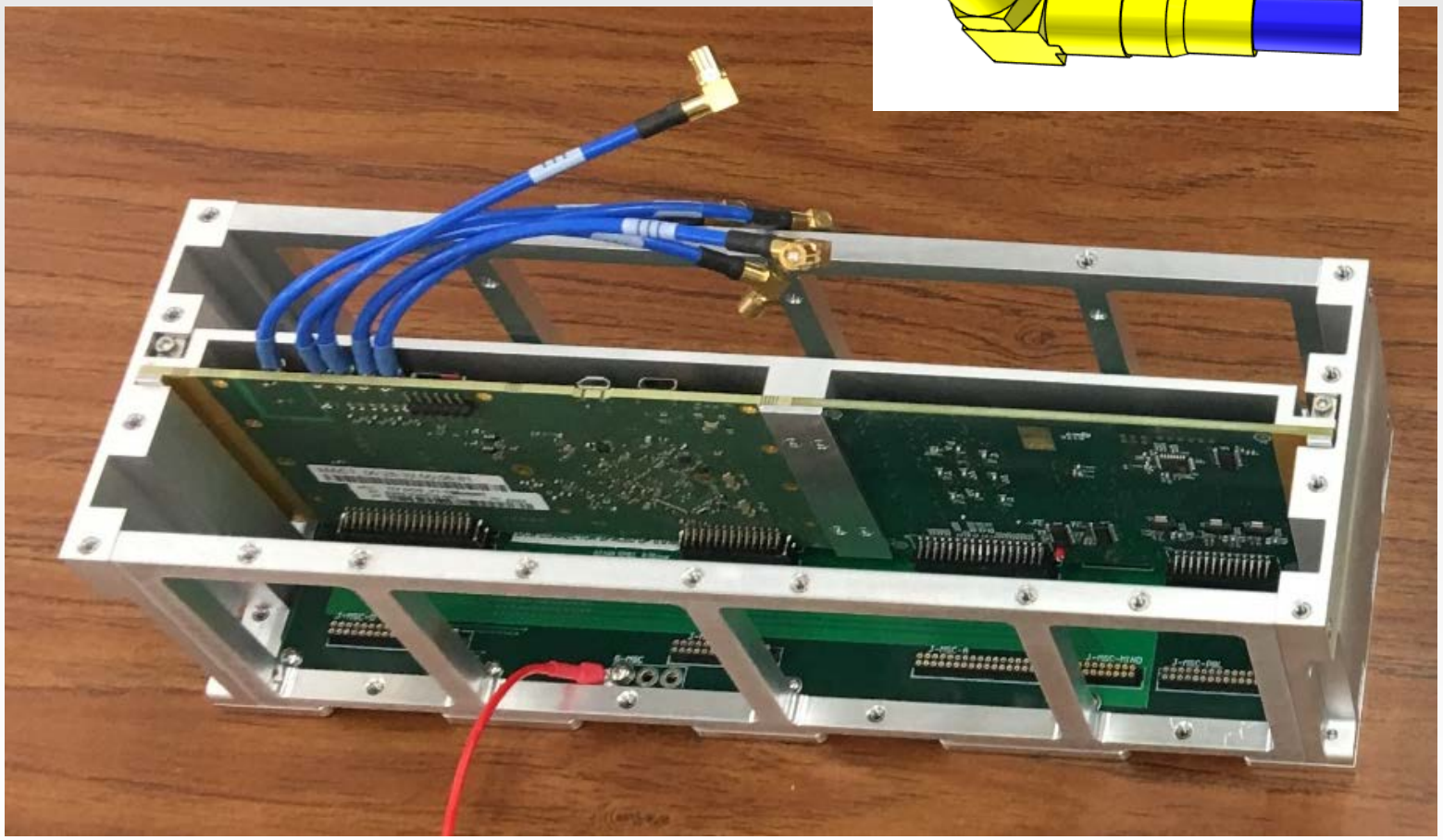

Mass Spec Control (MSC) board

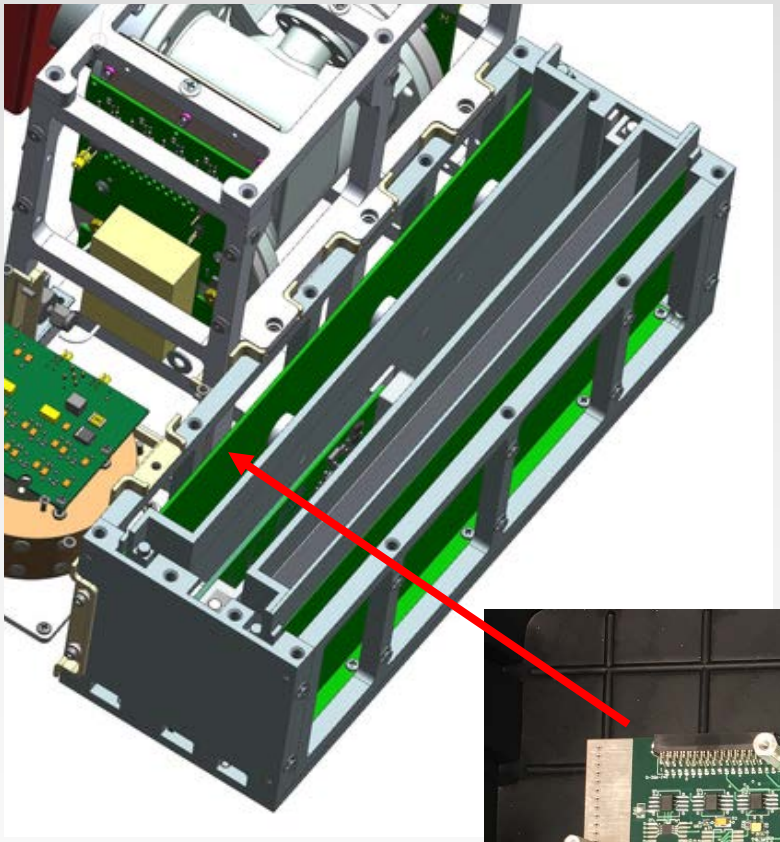

MSC

- Built in Space Physics Research Laboratory (SPRL), University of Michigan
- Layout for flight
- Rad hard 300 kRad
- High Voltage (3kV) for Micro Channel Plate detector
- Voltages for electron gun (constant and pulsing)
- Filament current

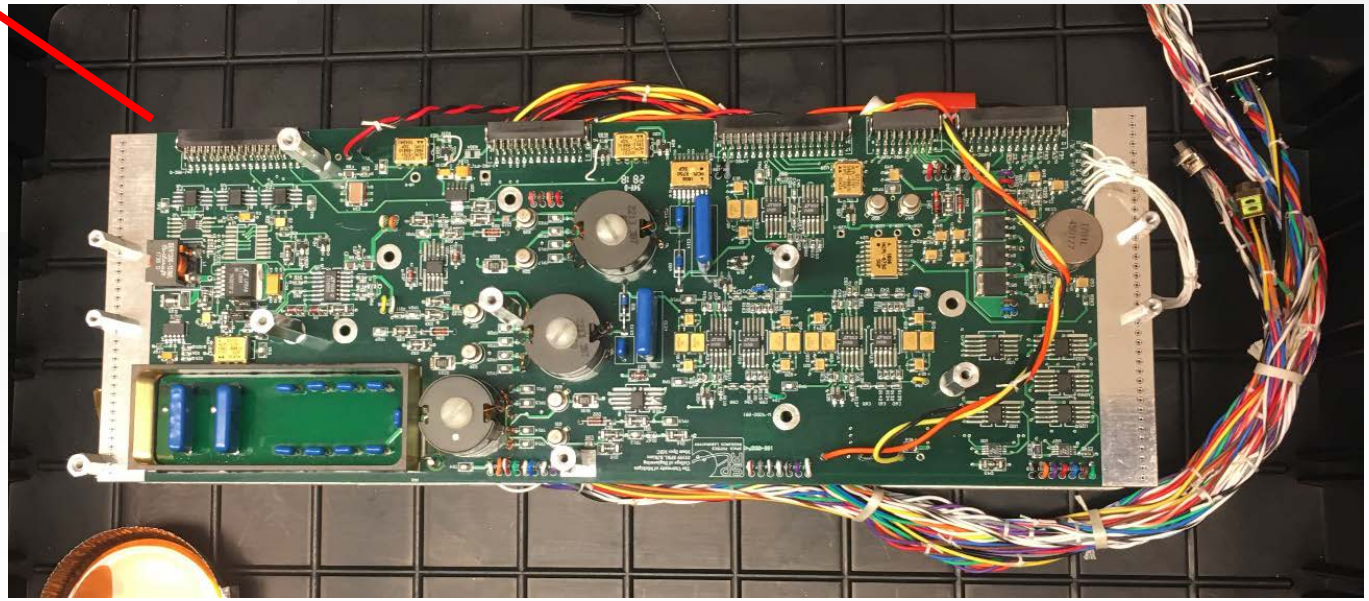

Mass Spec Control (MSC) HV power supply board before potting

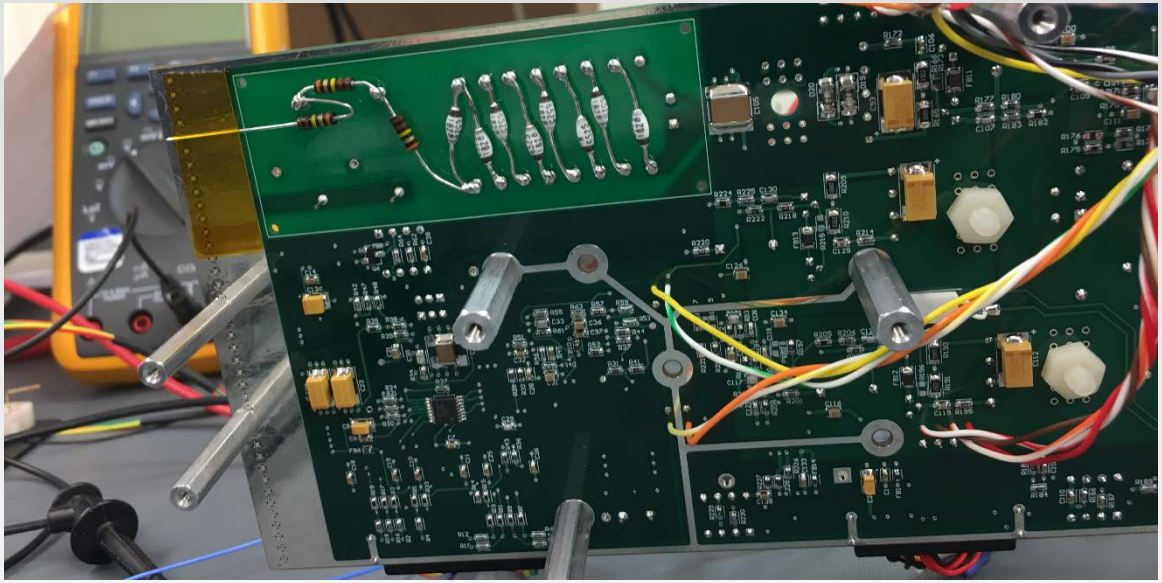

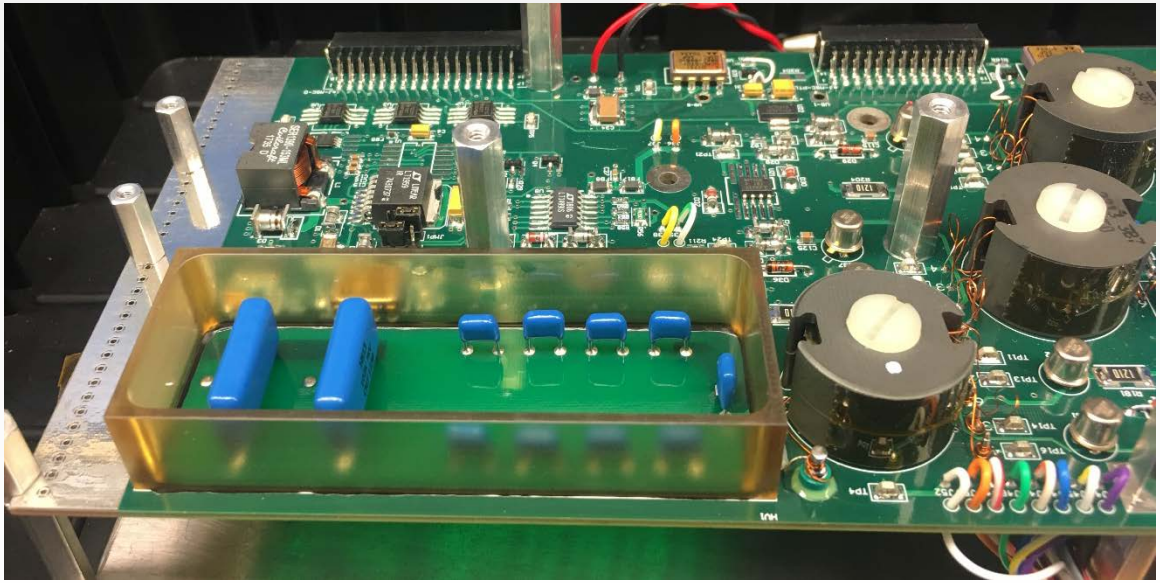

Integrating MSC

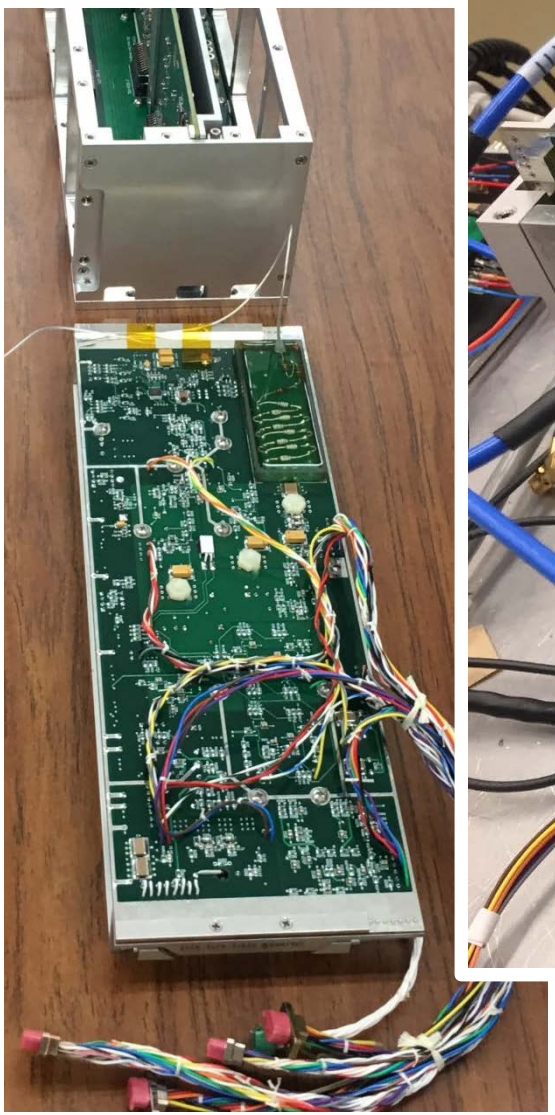

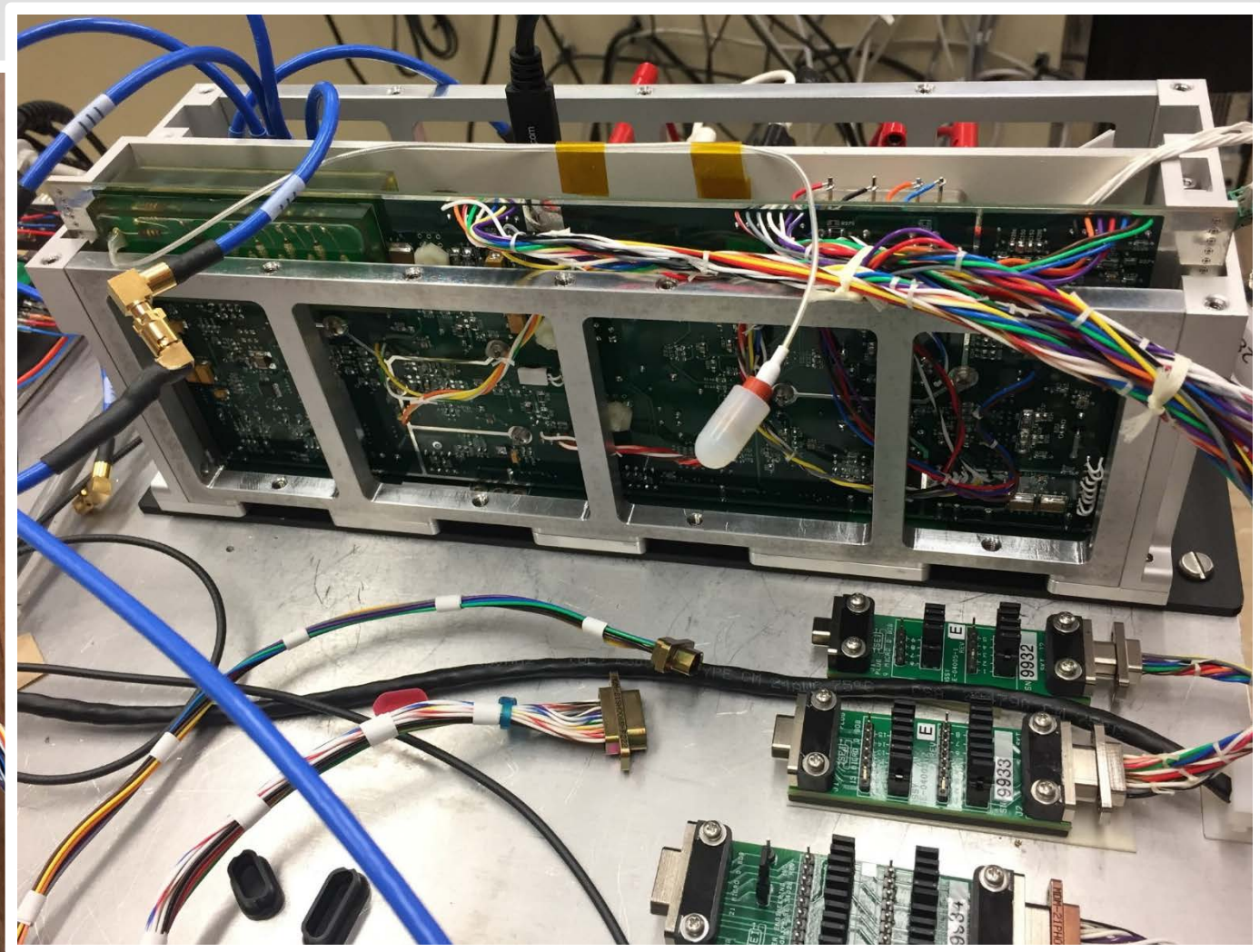

Electronics

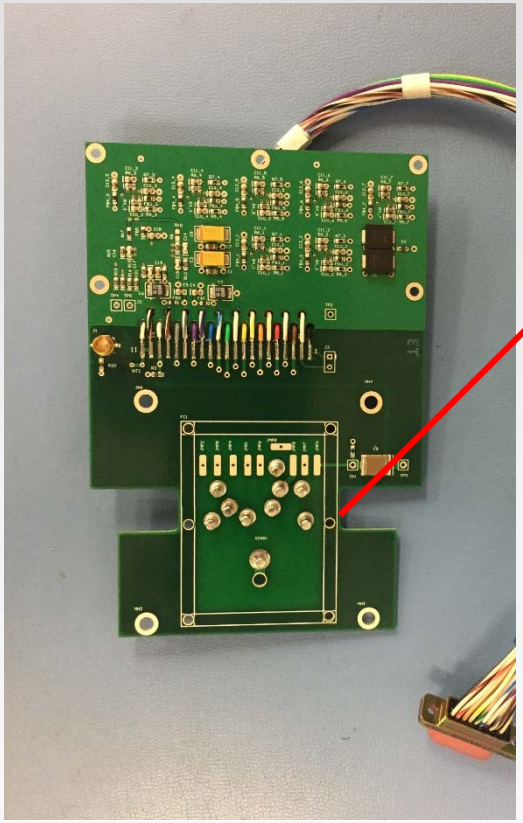

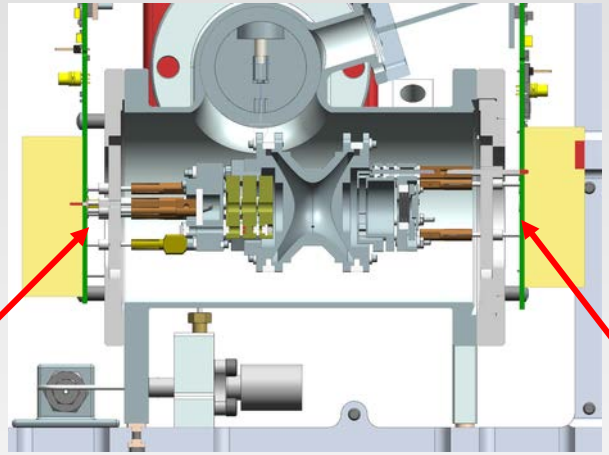

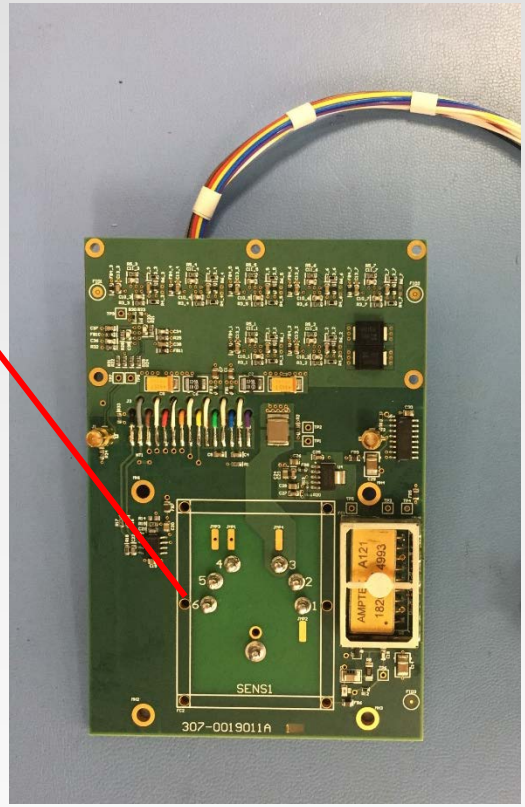

Top Cap PCB:

- e gun electrodes feedthrough
- 10 pins
- RF amp

Bottom Cap PCB:

- MCP detector feedthrough
- 7 pins
- RF amp
- A121 preamp

Assembly

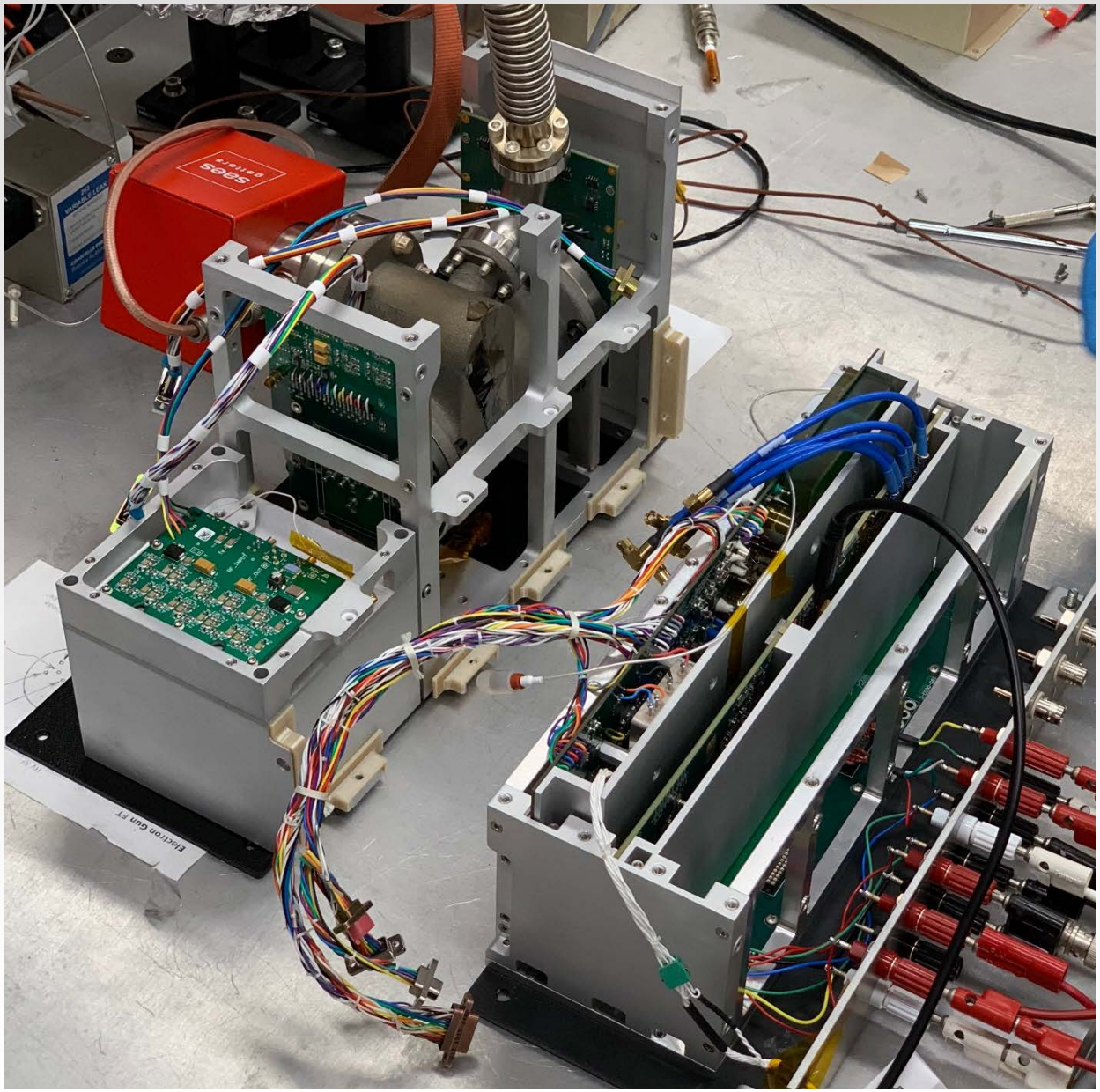

Assembly

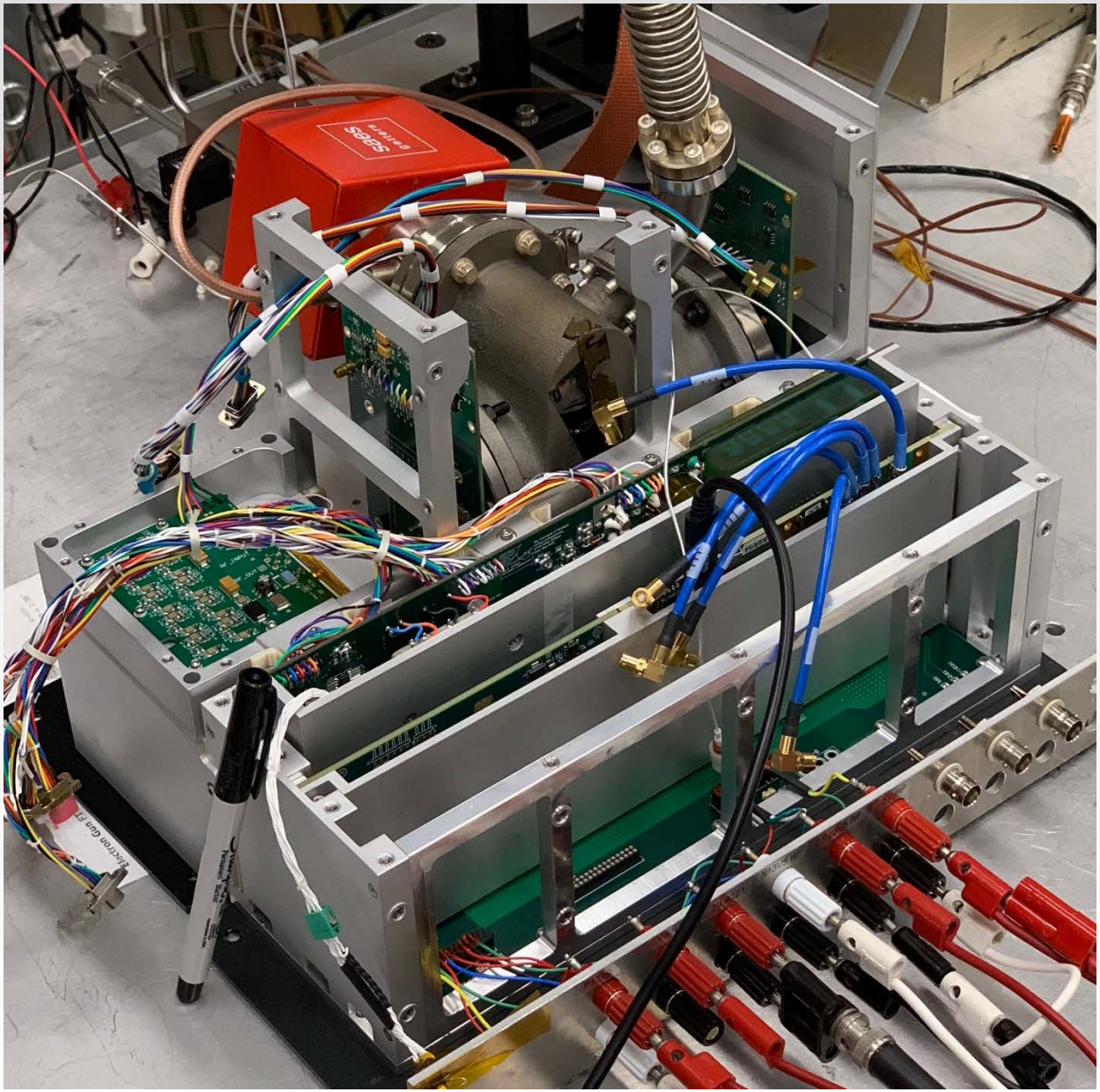

Thank you!

Reference herein to any specific commercial product, process, or service by trade name, trademark, manufacturer, or otherwise, does not constitute or imply its endorsement by the United States Government or the Jet Propulsion Laboratory, California Institute of Technology.

Conclusions

- CubeSat compatible: **3U** electronics, **4U** sensor, **1U** high Q RF coil. **8U total**
- 4 kg, 25W
- Rad Hard components up to 300 Krad
- All boards (except DCB and ADT) designed for flight
- Heatsink design for reliable operation in vacuum
- Battery pack module supports more than 2 hours of continuous measurements